# Elevated Expression of Acid-Sensing Ion Channel 3 Inhibits Epilepsy via Activation of Interneurons

**Qingqing Cao · Wei Wang · Juan Gu · Guohui Jiang · Kewei Wang · Zucai Xu · Jie Li · Guojun Chen · Xuefeng Wang**

**Abstract** Recent studies have indicated that acid-sensing ion channels may play a significant role in the termination of epilepsy. In particular, acid-sensing ion channel 3 (ASIC3) is expressed in the central nervous system and is most sensitive to extracellular pH. However, whether ASIC3 plays a role in epilepsy is unknown. In this study, qRT-PCR, Western blot, immunohistochemistry, double immunofluorescence labeling, and slice recordings were used. We first detected elevated ASIC3 expression patterns in the brains of temporal lobe epilepsy patients and epileptic rats. ASIC3 was expressed in neurons and glia in both humans and in an experimental model of epilepsy, and ASIC3 was colocalized with inhibitory GABAergic interneurons. By blocking ASIC3 with its antagonist APETx2, we observed that injected APETx2 shortened the latency to seizure and increased the incidence of generalized tonic clonic seizure compared to the control group in models of both pilocarpine- and pentylenetetrazole (PTZ)-induced seizures. Additionally, blocking ASIC3 significantly decreased the frequency of action potential (AP) firing in interneurons. Moreover, APETx2 significantly reduced the amplitudes and frequencies of miniature inhibitory postsynaptic currents (mIPSCs) while showed no differences with the APETx2 + bicuculine group and the bicuculline group. These findings suggest that elevated levels of ASIC3 may serve as an anti-epileptic mechanism via postsynaptic mechanisms in interneurons. It could represent a novel therapeutic strategy for epilepsy treatment.

**Keywords** Acid-sensing ion channel 3 · Temporal lobe epilepsy · APETx2 · Interneuron · GABA

Qingqing Cao and Wei Wang contributed equally to this work.

Q. Cao · W. Wang · J. Gu · Z. Xu · J. Li · G. Chen (✉) ·
X. Wang (✉)
Department of Neurology, The First Affiliated Hospital, Chongqing
Medical University, 1Youyi Rd, Chongqing 400016, China
e-mail: woodchen2015@163.com
e-mail: xfyp@163.com

Q. Cao
Department of Neurology, The People's Hospital of Bishan District,
82 Xinsheng Road, Chongqing 402760, China

G. Jiang
Department of Neurology, Affiliated Hospital of North Sichuan
Medical College, 63 Wenhua Road, Nanchong 637000, China

K. Wang
Department of Pharmacology, Peking University, 5 Summer Palace
road, Beijing 100871, China

X. Wang
Center of Epilepsy, Beijing Institute for Brain Disorders, Beijing,
China

## Introduction

Epilepsy is the third most common chronic brain disorder [1]. At present, approximately 50 million people worldwide have active epilepsy, with continuing seizures that require treatment. Of these, 20–40 % of patients with newly diagnosed epilepsy will become pharmacoresistant [2], and such cases are referred to as intractable epilepsy [3–5]. Temporal lobe epilepsy (TLE) is one of the major focal epilepsies, and 70–80 % of these cases develop into drug-refractory epilepsy [6]. However, the mechanisms underlying the pathogenesis of epilepsy, especially intractable epilepsy, are not well understood. Therefore, understanding critical anti-epileptic factors may lead to more effective treatments for epileptic patients [5].

Acid-sensing ion channels (ASICs) are $H^+$-gated, $Na^+$-permeable channels formed by the homomeric or heteromeric association of six different subunits [7], including ASIC1a (Waldmann et al. 1997b), ASIC1b [8], ASIC2a [9], ASIC2b [10], ASIC3 [11, 12], and ASIC4 [13]. These channels open when the extracellular pH decreases [14, 15]. ASIC3 is the

most H^{+} sensitive of the six isoforms and opens when the pH drops from 7.4 to 7.0, whereas the other ASICs are less sensitive to protons [16]. Additionally, ASIC3 is the only acid-sensitive ion channel that generates a sustained current in response to modest acidification within the limited range of extracellular pH from 7.3 to 6.7 [17], and ASIC3 shares aspects of permeation to and inhibition by $Ca^{2+}$, unlike the other ASICs [18]. However, ASIC3 is mainly distributed in sensory neurons, and functional ASIC3 channels are predominantly found in sensory neurons [19–21]. Moreover, ASIC3 transcripts and ASIC3 immunoreactivity have been detected in neurons of the hypothalamus [22], inferior colliculus [23], and suprachiasmatic nucleus [8] in the rat brain, and higher levels of ASIC3 was observed only in the midbrain and brainstem regions (Wu et al. 2010b). However, it remains unknown whether the central expression of ASIC3 plays a role in diseases of the nervous system, such as epilepsy.

In this study, we examined the expression and cellular localization of ASIC3 in the temporal cortex of patients with TLE. To rule out the possibility that anti-epileptic drugs (AEDs) affected ASIC3 expression, we investigated the dynamic changes in ASIC3 expression in the cortex and hippocampus using a rat model of epilepsy and also used the inhibitor APETx2 to evaluate the potential function of ASIC3 in epilepsy.

## Materials and Methods

### Human Brain Tissue Collection

The protocol used in this study complied with the guidelines for the conduct of research involving human subjects as established by the National Institutes of Health of China and the Committee on Human Research of Chongqing Medical University. Every patient or their relatives signed an informed consent form for the use of their data and tissues in our study, which was in accordance with the Declaration of Helsinki of the World Medical Association. The diagnosis of each patient is according to the criteria established by the International League Against Epilepsy (ILAE) [24].

All 25 samples (15 females and 10 males with mean age of 23.16±10.18 years, range 6–42 years) were chosen randomly from our epilepsy brain tissue bank. The mean time course was 9.68±6.68 years (range 1–22 years). All patients were refractory to the maximal doses of three or more AEDs, including phenytoin, valproic acid, carbamazepine, phenobarbital, topiramate, lamotrigine, oxcarbazepine, or levetiracetam. Table 1 summarizes the clinical features of the patients. The presurgical assessment consisted of performing a detailed medical history, a neurological examination, interictal and ictal electroencephalogram studies, neuropsychological testing, and magnetic resonance imaging (MRI). Video-EEG, sphenoidal electrode monitoring, and intraoperative electrocorticography were used to localize the epileptiform discharge zone during surgery. Then, the epileptiform discharge zones in the anterior temporal cortex were resected for treatment. Neuronal loss and gliosis were the most common histopathological findings in all samples. Ten control brain samples (six females and four males, mean age of 28.4±14.8 years, range 10–55 years) were obtained from patients who underwent therapeutic surgical resection for increased intracranial pressure due to head trauma. These patients had no history of epilepsy or other neurological diseases, and their histopathological findings were normal. Table 2 summarizes the clinical features of these patients.

### Rat Model of Epilepsy

The Institutional Animal Care and Use Committee of Chongqing Medical University approved all procedures used in this study. Male Sprague–Dawley rats (200–260 g body weight) were purchased from the Experimental Animal Center of Chongqing Medical University and housed in a temperature-controlled room with ad libitum access to food and water. All rats were randomly divided into eight subgroups ($n=8$ animals in each), consisting of animals that were sacrificed at 6 h, 24 h, 72 h, 1 week, 2 weeks, 1 month, and 2 months after the onset of status epilepticus (SE) induced by lithium-pilocarpine as well as a control group. Lithium chloride (127 mg/kg, intraperitoneally (i.p.), Sigma, USA) was injected 20 h prior to the first administration of pilocarpine. The experimental rats were initially injected with atropine methyl nitrate (1 mg/kg, i.p.), followed 30 min later by pilocarpine (50 mg/kg, i.p., Sigma, USA). Pilocarpine (10 mg/kg) was injected repeatedly every 30 min until the rats developed SE. Seizures were scored in each rat using the Racine seizure scale [25]. Only animals that entered into stage 4 were used for subsequent experiments. The control group received equivalent treatment, with the exception that they were injected with normal saline instead of pilocarpine. One hour later, diazepam (10 mg/kg, i.p.) was injected to control SE. The experimental rats were anesthesia by 3.5 % chloralic hydras (1 mL/100 mg) then sacrificed at 6 h, 24 h, 72 h, 1 week, 2 weeks, 1 month, and 2 months after SE, and the cortex and hippocampus were resected for our study.

### Tissue Processing

Both human and animal tissues were immediately divided into two portions. One portion was immediately frozen in liquid

**Table 1** Clinic characteristics of TLE patients

| Number | Age (year) | Sex (M/F) | Course (year) | AEDs before surgery | Resection tissue | Neuropathological diagnosis |
|---|---|---|---|---|---|---|
| 1 | 19 | M | 1 | VPA, CBZ, OXC | TNr | G |
| 2 | 32 | M | 6 | PHT, CBZ, VPA | TNr | NL, G |
| 3 | 17 | F | 7 | PHT, PB, VPA, LTG | TNL | NL, G |
| 4 | 19 | F | 10 | VPA, LTG, LEV | TNr | G |
| 5 | 6 | M | 5 | LEV, LTG, OXC | TNl | NL |
| 6 | 45 | M | 10 | CBZ, VPA, PHT, TPM | TNl | NL, G |
| 7 | 30 | M | 18 | PHT, VPA, TPM, PB | TNl | NL, G |
| 8 | 7 | F | 1 | LEV, LTG, TPM | TNr | G |
| 9 | 29 | F | 22 | VPA, CBZ, PHT, LTG | TNr | NL, G |
| 10 | 26 | M | 2 | VPA, TPM, LTG | TNl | NL |
| 11 | 15 | M | 3 | VPA, LTG, OXC, LEV | TNr | NL, G |
| 12 | 16 | F | 15 | VPA, CBZ, PHT | TNl | NL, G |
| 13 | 30 | M | 10 | VPA, PHT, LTG, LEV | TNr | NL, G |
| 14 | 42 | F | 22 | CBZ, VPA, TPM | TNl | G |
| 15 | 35 | M | 6 | VPA, LTG, TPM | TNl | NL |
| 16 | 26 | M | 14 | CBZ, VPA, TPM | TNr | NL, G |
| 17 | 30 | M | 10 | VPA, CBZ, PHT, OXC | TNr | G |
| 18 | 15 | M | 14 | VPA, LTG, OXC, LEV | TNl | NL |
| 19 | 17 | F | 4 | TPM, LTG, VPA | TNr | G |
| 20 | 14 | M | 7 | TPM, OXC, LEV | TNl | NL, G |
| 21 | 9 | F | 1 | LEV, TPM, VPA | TNl | G |
| 22 | 18 | F | 16 | VPA, CBZ, PB, LTG | TNr | G |
| 23 | 32 | F | 7 | VPA, PHT, CBZ, OXC | TNl | NL, G |
| 24 | 24 | M | 20 | VPA, CBZ, PHT, TPM | TNl | NL, G |
| 25 | 26 | M | 9 | PHT, CBZ, VPA, PB | TNl | NL, G |

*F* female, *M* male, *AEDs* anti-epileptic drugs, *CBZ* carbamazepine, *LTG* lamotrigine, *LEV* levetiracetam, *OXC* oxcarbazepine, *PHT* phenytoin, *PB* phenobarbital, *TPM* topiramate, *VPA* valproic acid, *TN* temporal neocortex, *r* right, *l* left, *NL* neuronal loss, *G* gliosis

nitrogen and then stored at −80 °C for Western blot analysis and quantitative real-time PCR. The remaining tissue was fixed in 4 % phosphate-buffered formalin for 48 h. Then, one portion of the remaining tissue was frozen and cut into 10-µm-thick sections with a cryostat for double immunofluorescence labeling analysis and stored at −20 °C, whereas the other portion was embedded in paraffin and divided into 5-µm-thick sections for immunohistochemistry analysis. Additionally, two sections from each specimen were processed for hematoxylin-eosin staining.

Western Blot Analysis

Total protein was extracted from homogenized brain tissue using the enhanced RIPA lysis buffer (Beyotime Institute of Biotechnology, Jiangsu, China) according to the manufacturer's protocols. Then, 50 µg of extracted protein was separated on an 8 % polyacrylamide Tris–HCl gel and transferred to a PVDF membrane (Millipore, Billerica, MA, USA, pore size 0.45 µm). After incubating with primary rabbit polyclonal anti-ASIC3 antibody (1:3500, catalogue number ab77383, Abcam,

Cambridge) or primary mouse monoclonal anti-GAPDH antibody (1:1000, Beyotime), the membranes were reacted with goat anti-rabbit or goat anti-mouse peroxidase-conjugated secondary antibody (1:2000, Beyotime), respectively, at 37 °C for 1 h. The resulting protein bands were visualized using an

**Table 2** Clinical characteristics of control group

| Number | Age (year) | Sex (F/M) | Etiology diagnosis | Resection tissue | Tissue pathology |
|---|---|---|---|---|---|
| 1 | 10 | M | Trauma | TNr | N |
| 2 | 12 | F | Trauma | TNl | N |
| 3 | 22 | M | Trauma | TNl | N |
| 4 | 36 | M | Trauma | TNl | N |
| 5 | 22 | F | Trauma | TNr | N |
| 6 | 30 | F | Trauma | TNr | N |
| 7 | 47 | M | Trauma | TNl | N |
| 8 | 55 | F | Trauma | TNr | N |
| 9 | 34 | M | Trauma | TNl | N |
| 10 | 16 | M | Trauma | TNr | N |

*F* female, *M* male, *TN* temporal neocortex, *r* right, *l* left, *N* normal

enhanced chemiluminescence substrate kit (Beyotime) and were scanned and analyzed with Quantity One software (Bio-Rad Laboratories). Optical density values were normalized to the corresponding value of GAPDH.

### Quantitative real-time PCR

Total RNA was extracted using RNAiso Plus (TaKaRa Biotechnology Co. Ltd., Dalian, China). Contaminated genomic DNA (gDNA) was removed, and RNA was reverse-transcribed using the PrimeScript RT reagent kit with gDNA Eraser according to standard protocols. Quantitative real-time PCR was performed using an ABI Prism 7500 Fast Real-Time PCR system (Bio-Rad Laboratories). Each reaction was performed in a volume of 20 μL containing 1 μg cDNA, 10 μL SYBR Green PCR Master Mix (Applied Biosystems), and 10 μM of each (forward and reverse) PCR primer. All reactions were performed in triplicate. Levels of the various messenger RNAs (mRNAs) were normalized to those of the rat housekeeping gene β-actin. The following forward and reverse primers were used: ASIC3, 5′-aaggaacagtgggacctgacc-3′and 5′-gggctaaggaggctaagatagga-3′, and β-actin, 5′-ccacgaaactaccttcaactcc-3′ and 5′-gtgatctc cttctgcatcctgt-3′. The relative expression level of ASIC3 mRNA in TLE patients compared to the controls was calculated using the $2^{-\Delta\Delta Ct}$ method [26].

### Immunohistochemistry

We performed immunohistochemistry using streptavidin/peroxidase kits (Zhongshan Golden Bridge Biotechnology Co. Ltd., Beijing, China), according to the protocols recommended by the manufacturer. Tissue sections were immersed in xylene for 20 min for deparaffinizing, and then rehydrated in graded ethanol for 5 min at each grade. Then, sections were blocked with 0.3 % $H_2O_2$ for 10 min followed by antigen retrieval. Sections were immersed in 10 mM sodium citrate buffer and heated (92–98 °C) in a microwave oven for 20 min. Nonspecific binding was blocked with goat serum for 30 min at 37 °C. Then, sections were incubated with primary rabbit polyclonal anti-ASIC3 antibody (1:200) at 4 °C overnight. Then, the sections were incubated with biotinylated goat anti-rabbit secondary antibody and avidin–biotin complex (ABC) working solution, after which point the sections were incubated with 3,3-diaminobenzidine (DAB) (Zhongshan) for 3 min. As a negative control, primary antibody was replaced with phosphate-buffered saline (PBS). Counterstaining was carried out with Harris's hematoxylin. An Olympus PM20 automatic microscope (Olympus, Osaka, Japan) and TC-FY-2050 pathology system (Yuancheng Inc., Beijing, China) were used to collect the images. Image-Pro plus 6.0 software (Media Cybermetrics Inc., USA) was used for

the semiquantitative analysis of ASIC3 expression. The mean optical density (OD) of each visual field was automatically calculated to measure the differences between the TLE group and the control group.

### Double Immunofluorescence Labeling

The sections were fixed in acetone for 20 min, and then antigen retrieval was performed using microwave heating. The tissue was permeabilized with 0.4 % triton X-100 for 15 min, followed by incubation with 5 % goat serum (Zhongshan) for 30 min at 37 °C. Then, sections were then incubated with a mixture of rabbit polyclonal anti-ASIC3 antibody (1:50) and mouse monoclonal anti-neuron-specific enolase (NSE) antibody (1:100, Zhongshan) or anti-glial fibrillary acidic protein (GFAP) antibody (1:100, Wuhan Boster Biological Technology, Wuhan, China) or anti-GAD67 antibody (1:100, catalogue number ab26116, Abcam, Cambridge) at 4 °C overnight. Subsequently, the sections were incubated with DyLight488-Conjugated AffiniPure Goat Anti-Rabbit IgG (1:200, Zhongshan) and DyLight594-Conjugated AffiniPure Goat Anti-Mouse IgG (1:200, Zhongshan) in a darkroom for 90 min at 37 °C and mounted in 1:1 glycerol/PBS. Fluorescence was examined by laser scanning confocal microscopy (Leica Microsystems Heidelberg GmbH, Germany) using an Olympus IX 70 inverted microscope (Olympus) equipped with a Fluoview FVX confocal scan head.

### Behavioral Assays

To evaluate the role of ASIC3 in seizures, we injected APETx2 (catalogue number RTA-100, Alomone labs), the selective blocker of ASIC3, or artificial cerebral spinal fluid (ACSF, 124 mM NaCl, 3 mM KCl, 1.2 mM $NaH_2PO_4$, 1.2 mM $MgSO_4$, 2 mM $CaCl_2$, and 26 mM $NaHCO_3$) into rats to record the differences between the experimental group and the control group according to the Racine seizure scale [25]. Right-lateral, intracerebroventricular (ICV) guide cannulae were implanted in anesthetized by 3.5 % chloralic hydras (1 mL/100 mg) rats (AP −1.0 mm, ML −1.5 mm, DV −3.25 mm).We injected 5 μL of APETx2 in ACSF (5 or 10 μM), ACSF alone or normal saline 2 days later into rats using a 10-μL micropipette connected to an injection tube (over 10 s). Following injection with pilocarpine (50 mg/kg, i.p.), the rat's behavior was scored as above, and only scores exceeding stage 4 were considered successful and were incorporated into our study (5 μM APETx2 + pilocarpine (pilo), n=10; 10 μM APETx2 + pilo, n=9; ACSF + pilo, n=8; control + pilo, n=9). Lithium chloride (127 mg/kg, i.p.) was injected 20 h prior to the administration of pilocarpine. The pilocarpine model of epilepsy in rodents

**Table 3** Comparison of clinical data in patients with TLE and the control group

| Variable | TLE group (n=25) | Control group (n=10) | P value |
|---|---|---|---|
| Course (year) | 9.68±6.68 | NA | NA |
| Age (year) | | | |
| Mean±SD | 23.16±10.18 | 28.4±14.86 | 0.238 |
| Range (year) | 6–42 | 10–55 | NA |
| F/M ratio | 10:15 | 4:6 | 0.652 |

P values were counted using an independent samples t test (age) or a Fisher's exact test (male/female ratio). P<0.05 was considered significant

F female, M male, NA not applicable

is a commonly used model to study temporal lobe epilepsy [27]. Pentylenetetrazole (PTZ) kindling is the most widely accepted animal model for studying the effects of novel antiepileptic molecules [28]. So, we performed experiments with PTZ (75 mg/kg, i.p.) substituted for

pilocarpine and without injection of lithium chloride. A trained observer who was blinded to experiment scored the seizure severity.

### In Vivo Multichannel Electrophysiological Recording and LFP Analysis

Left-lateral ICV guide cannulae were implanted in anesthetized by 3.5 % chloralic hydras (1 mL/100 mg) rats (AP −1.0 mm, ML 1.5 mm, DV −3.25 mm). A intracranial electrophysiological recording microwire array (2×4 array of platinum-iridium alloy wire, each with 25-µm diameter, Plexon, Dallas, TX) was implanted into the right dorsal hippocampus (AP −3.2 mm, ML −2.5 mm, DV −2.6 mm) and fixed on the skull by dental cement. Animals were recovered from surgery for several days before the electrophysiological recording. Local field potentials (LFPs) were recorded using OmniPlex® D neural Data Acquisition System (Plexon, Dallas, TX). The signals were filtered (0.1–1000 Hz), preamplified (1000×),
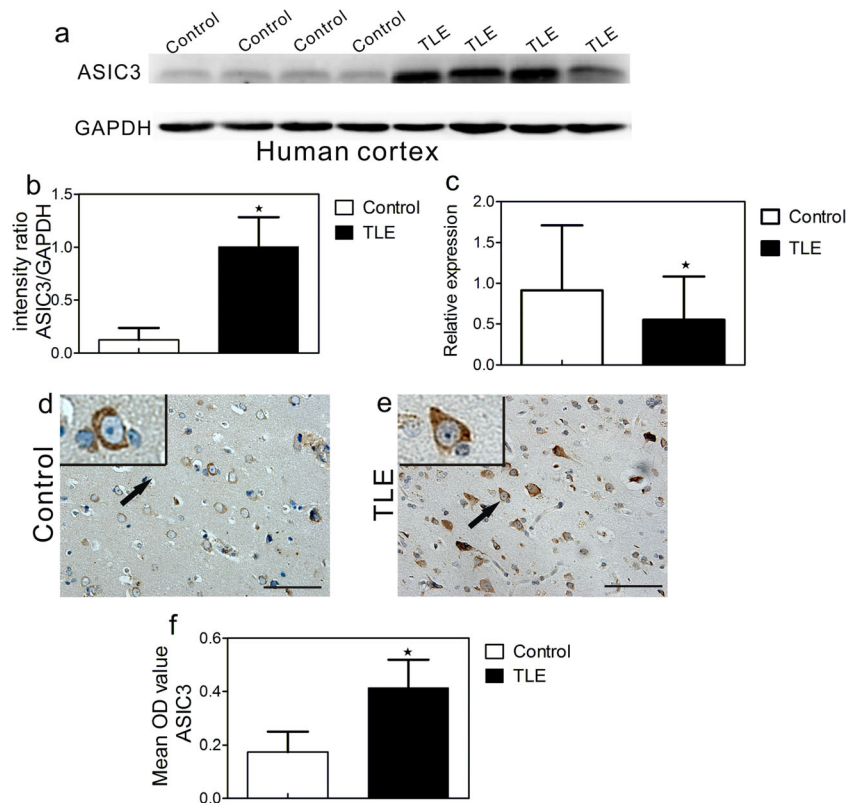


**Fig. 1** Altered expression of ASIC3 in patients with TLE. **a** Representative bands of ASIC3 and GAPDH. ASIC3 expression was strong in the temporal cortex of TLE patients (lanes 5–8), whereas it was relatively weak in the controls (lanes 1–4). **b** Comparison of the intensity ratio indicated significantly increased ASIC3 expression in the TLE group (n=25) as compared to the control group (n=10) (★P<0.05). **c** The mRNA expression of ASIC3 in the patients with TLE (n=15) was significantly decreased compared to the controls (n=10) (★P<0.05). **d** Faint staining of ASIC3 in the temporal cortex of control subjects. **e** Strong staining of ASIC3 in the temporal cortex of TLE patients. **f** Comparison of the mean OD values indicated significantly higher expression of ASIC3 in patients with TLE (n=15) as compared to the control subjects (n=10) (★P<0.05). Black arrows show the ASIC3-positive cells. Scale bars 50 µm

and digitized at 4 kHz. The LFP analysis was conducted using Neuro Explorer v4.0 (Plexon, Dallas, TX). Electrophysiological data were reviewed and scored by two laboratory assistants who did not know the experimental program. Seizures were induced in rats by lithium chloride-pilocarpine or PTZ. APETx2 (10 μm) or saline was injected into the lateral ventricle by microinjection cannula. Thirty minutes later, convulsant drug (pilocarpine or PTZ) was injected into abdomen, and the electrophysiological recording was continuously recorded more than 70 min (pilocarpine) or 10 min (PTZ). An electrophysiological seizure were defined as high amplitude (>2 times the baseline), high frequency (>5 Hz), lasting longer than 5 s [29].

Slice Recordings and Analysis

Experiments were performed according to standard methods on rat brain slices prepared using a vibratome. Male Sprague–Dawley rats (6–7 weeks of age) were anesthetized with 3.5 % chloral hydrate and then transcardially perfused with a high-$Mg^{2+}$/low-$Ca^{2+}$ solution (4.9 mM $MgSO_4$, 0.5 mM $CaCl_2$, 126 mM NaCl, 5 mM KCl, 1.25 mM $NaH_2PO_4$, 27.7 mM $NaHCO_3$, 10 mM dextrose, 1.1 mM $MgCl_2$, pH 7.35) chilled to 4 °C. Then, the rats were sacrificed by decapitation, and their brains were removed and washed in cold ACSF. Slices were sectioned in a horizontal plane from the hippocampus (350 μm), followed by incubation in prewarmed, oxygenated (95 % $O_2$/5 % $CO_2$) ACSF for at least 1 h prior to testing.

For extracellular recordings, glass electrodes (3–5 MΩ) were filled with ACSF and placed in the CA3 cell layer. Spontaneous epileptiform activity was induced by a convulsant ACSF containing 0 $Mg^{2+}$.

To measure cell excitability, the whole-cell current-clamp technique was used to record action potentials (AP) in CA1 region. (Chen et al. 2006). The pipettes (3–5 MO polished glass pipettes) contained 5 mM NaCl, 90 mM potassium gluconate, 15 mM KCl, 1 mM $MgCl_2$, 10 mM EGTA, 60 mM HEPES, and 3 mM $Na_2ATP$, adjusted to pH 7.3 with KOH. Cells were not used if the initial resting membrane potential was more depolarized than −60 mV. For spontaneous firing recordings, a small depolarizing current was applied to adjust the interspike potential to −60 mV. To evoke seizure activity, we replaced normal ACSF with ACSF lacking $MgSO_4$. After recording 2 min of epileptiform spike, we reduced the pH to 6.6 by buffering the solutions with HEPES. We measured pH in the recording chamber both before and during the infusion of ACSF (pH 6.6). The effects of low pH were then recorded for 2 min, after which time we infused ACSF (pH 6.6) containing 63 nM APETx2 and recorded the epileptiform spike. To quantify epileptiform activity,
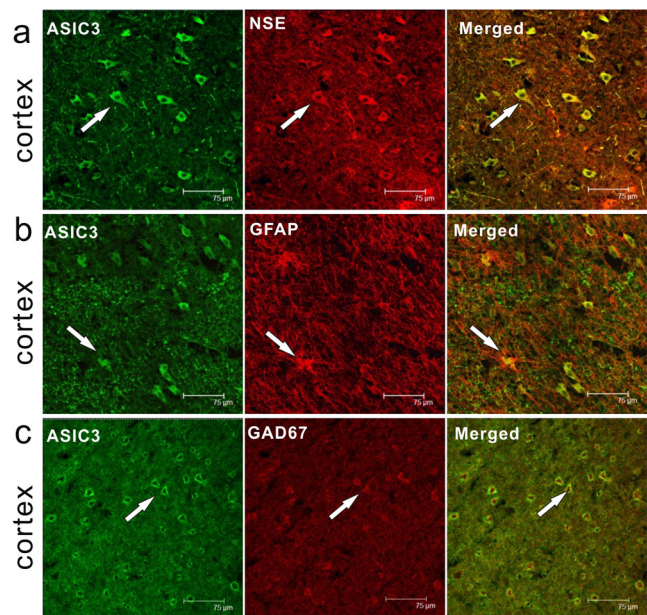
**Fig. 2** Double immunofluorescence labeling for ASIC3 in TLE patients. Representative pictures showing the coexpression of ASIC3 and NSE (**a**), ASIC3 and GFAP (**b**), and ASIC3 and GAD67 (**c**) in the cortex of patients with TLE. ASIC3 (*green*), NSE or GFAP or GAD67 (*red*), merged (*yellow*). *White arrows* show ASIC3/NSE/GFAP/GAD67-positive cells. *Scale bars* 75 μm (color figure online)

we used a previously described method. Using the Clampfit10.3 software, we quantified the total number of APs before and after infusion with ACSF containing APETx2. Inhibitory neurons and pyramidal neurons of the CA1 region were identified according to their location, morphology, and firing pattern (Parra et al. 1998).

To record miniature inhibitory postsynaptic currents (mIPSCs), the recording electrode was filled with internal solution (containing (in mM) CsCl, 100; HEPES, 10; $MgCl_2$, 1; EGTA, 1; N-methyl-D-glucamine (NMG), 30; MgATP, 5; $Na_2GTP$, 0.5; phosphocreatine, 12, pH 7.2–7.3, 270–280 mOsm). The recordings were done at a holding potential of −70 mV in the presence of 6,7-dinitroquinoxaline-2,3(1H,4H)-dione (DNQX) (10 μM), dL-2-amino-5-phospho-novaleric acid (DL-APV) (50 μM), and tetrodotoxin (TTX) (1 μM). The recorded mIPSCs were analyzed by Mini Analysis 6.0.1 and Clampfit10.3.

For assessments of presynaptic GABAergic contributions, a paired pulse protocol executed for two stimuli at an interpulse interval of 50 ms in the presence of DNQX (10 μM) and DL-APV (50 μM) to block glutamatergic transmission. Each current response is averaged from ten repetitive stimuli at a frequency of 0.1 Hz. The paired pulse ratio (PPR) was defined as the amplitude of the second response to the amplitude of the first response. Analysis was performed with Clampfit 10.3.
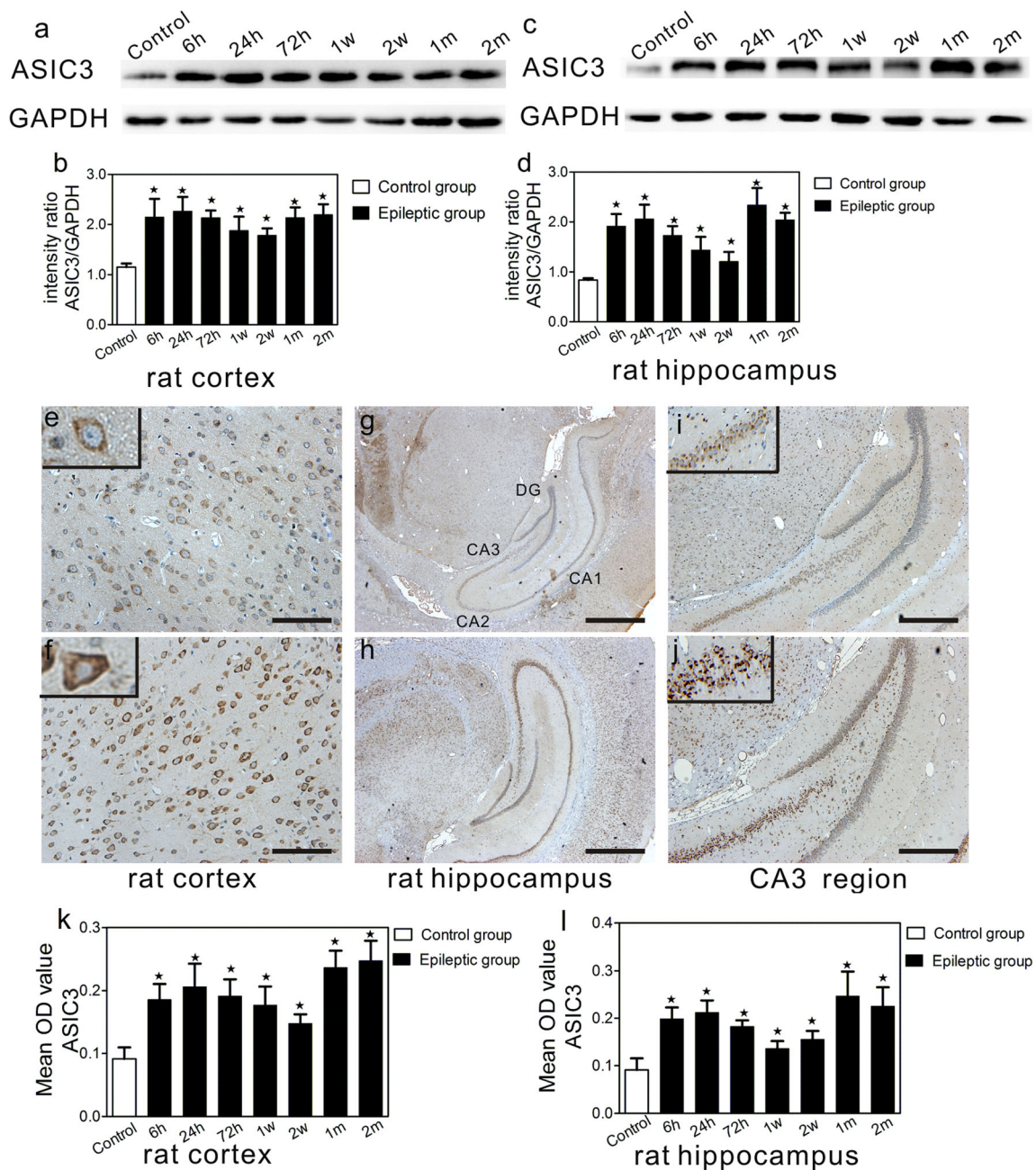
**Fig. 3** Representative Western blot image for ASIC3 in experimental rats. **a** In the cortex, ASIC3 protein was detected as a band at approximately 59 kDa, and GAPDH was detected as a band at 36 kDa. Lane 1 represents the normal rat sample, and lanes 2–8 represent different time points after seizures. **b** A distinctly stronger immunoblot was observed in experimental rats at each time point (n=5 of each) compared to the controls (n=5) (★P<0.05). **c** Representative Western blot image of ASIC3 and corresponding GAPDH expression in the hippocampus. **d** Comparison of the intensity ratio of ASIC3 expression between the control (n=5) and epileptic rats at different time points (n=5 of each) after kindling in the hippocampus (★P<0.05). Faint staining was evident in the control group in the cortex (**e**), DG (**g**), and CA3 region (**i**), whereas **f**, **h**, and **j** show strong staining in epileptic rats. **k**, **l** A comparison of the mean OD value for ASIC3 in the cortex and hippocampus, respectively, between epileptic rats and control subjects (★P<0.05). *Black arrows* show the ASIC3-positive cells. *Scale bars* **e**, **f** 50 μm; **g**, **h** 200 μm; **i**, **j** 100 μm

When a whole cell recording configuration was achieved, a Multiclamp 700B amplifier (Axon, USA) was used for the recording. Signals were sampled at 10 kHz and filtered at 2 kHz. Data were collected after currents had been stable for 5–10 min. Results were discarded if the series resistance changed by >15 %.
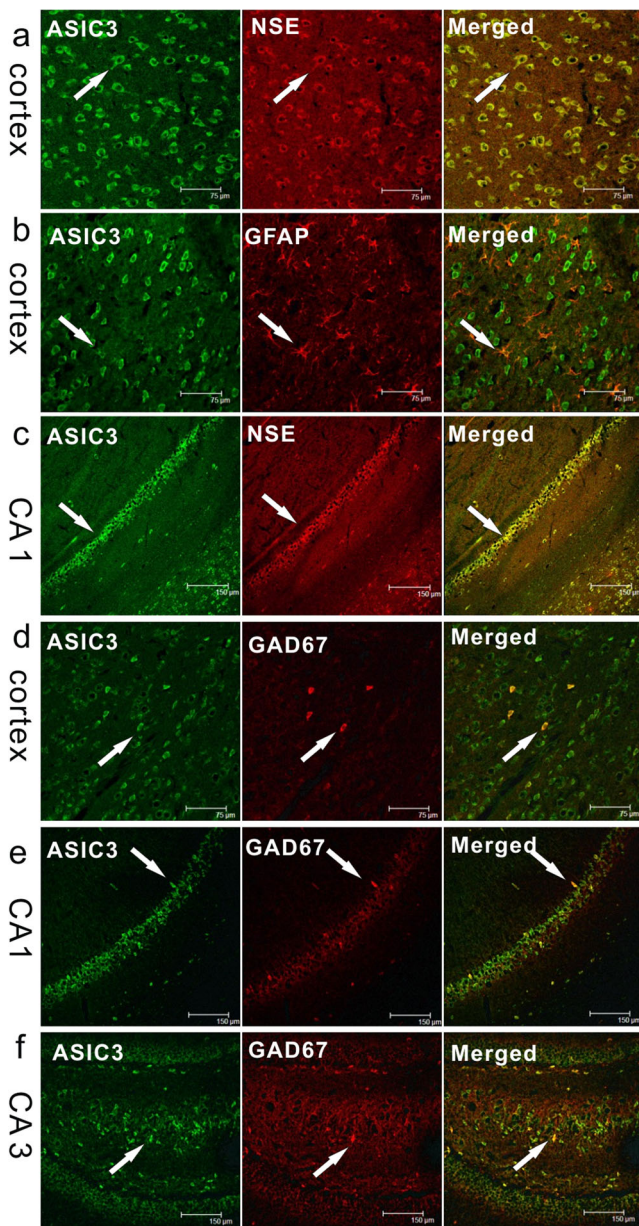
**Fig. 4** Double immunofluorescence labeling for ASIC3 in epileptic rats ASIC3 (*green*) and NSE (*red*) were coexpressed (merged) in the cortex of an epileptic rat (**a**) and CA1 region of an epileptic rat (**c**). ASIC3 (*green*) and GFAP (*red*) were coexpressed (merged) in the soma in the temporal cortex of an epileptic rat (**b**). ASIC3 (*green*) and GAD67 (*red*) were colocalized (merged) in the cortex (**d**), CA1 region (**e**), and CA3 region of epileptic rats (**f**). *White arrows* show ASIC3/NSE/GFAP/GAD67-positive cells. *Scale bars* **a**, **b**, **d**, **e** 75 μm; **c**, **f** 150 μm (color figure online)

## Results

All the values are presented as mean±SD. Differences were considered statistically significant with a *P* value <0.05.

Comparison of Clinical Data in Patients with TLE and Controls (see Table 3)

### Altered ASIC3 Expression in the Temporal Cortex of Patients with TLE

ASIC3 protein was detected as a single band at approximately 59 kDa, with GAPDH detected at 36 kDa (Fig. 1a). ASIC3 protein expression was normalized by calculating the intensity ratio of the bands according to the corresponding level of GAPDH. The intensity ratio was significantly increased in TLE patients (mean intensity ratio 1.005±0.279) as compared to controls (0.1223±0.1129) (*P*<0.05) (Fig. 1b). Next, we examined the expression of ASIC3 mRNA using quantitative real-time PCR. The relative expression level of ASIC3 mRNA in control patients was 1.79 times greater than in TLE patients, as calculated using $2^{-\Delta\Delta Ct}$ method (*P*<0.05) (Fig. 1c). By immunohistochemical staining, we observed faint ASIC3 staining in sections from the control group (Fig. 1d), whereas strong staining was detected in TLE samples (Fig. 1e). Significantly elevated ASIC3 protein expression was detected in TLE patients (mean OD value 0.414±0.105) compared to the control group (0.173±0.075) (*P*<0.05) (Fig. 1f) using an independent samples *t* test.

### Cellular Localization of ASIC3 in the Cortex of Patients with TLE

ASIC3 protein was mainly expressed in the neuronal cytomembrane and cytoplasm of the temporal cortex tissue of control and TLE patients, as shown by colocalization with the neuron marker NSE (Fig. 2a). ASIC3 was also expressed in glia, but it was only expressed in the soma and not in the dendrites. As shown by colocalization with the astrocyte marker GFAP, only the soma staining merged with that for ASIC3 (Fig. 2b). To explore the function of ASIC3 in epilepsy, we observed that ASIC3 was colocalized with GAD67, a marker for the production of the inhibitory neurotransmitter GABA (Fig. 2c).

### Elevated ASIC3 Expression in the Cortex and Hippocampus of Epileptic Rats

We performed experiments using a rat model of epilepsy, and the results were in accordance with our findings from TLE patients. ASIC3 was detected as a band of protein at approximately 59 kDa, whereas GAPDH was detected at 36 kDa (Fig. 3a, c). Furthermore, ASIC3 expression began to increase from 6 to 72 h after seizure, demonstrated a slight decrease at 1 and 2 weeks after seizure, then increased again at 1 and 2 months after seizure and was maintained at a relatively high
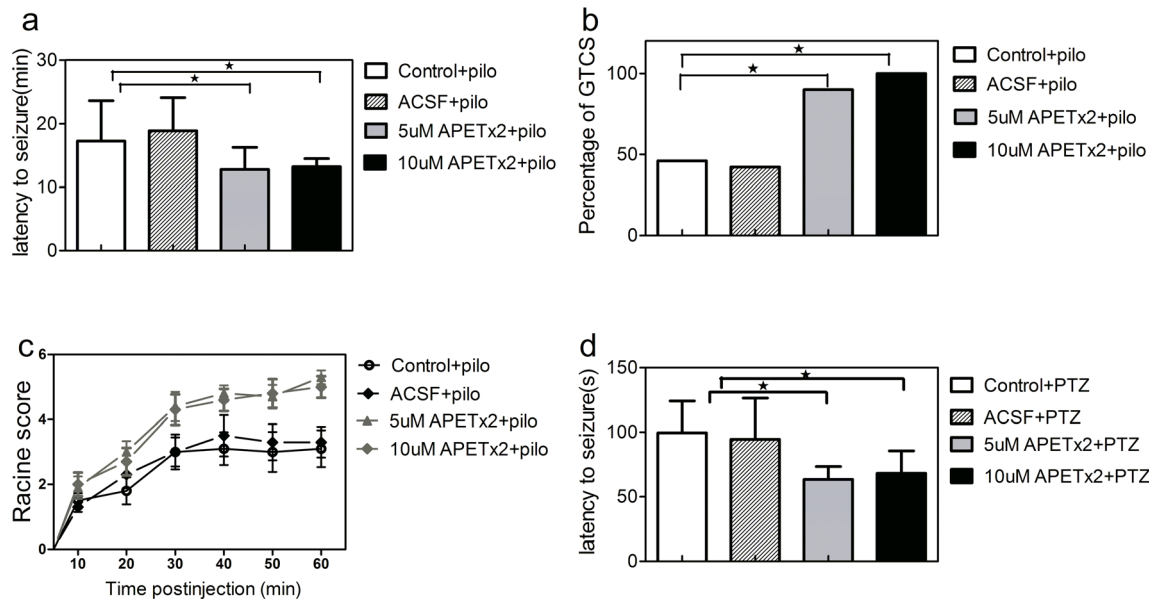
**Fig. 5** Effect of the ASIC3 inhibitor on seizure severity. **a** APETx2 significantly shortened the latency to seizure in 5 μM APETx2-treated (★$P<0.05$) and 10 μM APETx2-treated rats (★$P<0.05$) compared to the controls ($n=8$) in a model of pilocarpine-induced seizures. **b** Comparison of the incidence of GTCS between 5 μM APETx2-treated (★$P<0.05$),

10 μM APETx2-treated (★$P<0.05$), and controls ($n=10$ of each). **c** The rats treated with APETx2 developed more severe seizures compared to the controls over time (★$P<0.05$). **d** Rats treated with APETx2 demonstrated shorter latency to seizure after PTZ injection

level during the chronic stage both in the cortex (Fig. 3b) ($P<0.05$) and the hippocampus (Fig. 3d) ($P<0.05$). As shown in Fig. 3e, g, i, only faint staining for ASIC3 was detected in control samples, whereas strong staining for ASIC3 was detected in the temporal cortex (Fig. 3f), hippocampus (Fig. 3h), and CA3 pyramidal cell layers (Fig. 3j). Moreover, we confirmed the elevated expression of ASIC3 in the cortex (Fig. 3k) ($P<0.05$) and hippocampus (Fig. 3l) ($P<0.05$) of epileptic rats; expression was increased during the acute stage (6, 24, and 72 h), decreased in the silent stage (1 and 2 weeks), although still exceeding that in the control group, and was then increased again during the chronic stage (1 and 2 months). The mean OD values of ASIC3 for the control and epileptic rats were significantly different, according to one-way ANOVA followed by Tukey's HSD (Honestly Significant Difference) post hoc multiple comparison test.

Cellular Localization of ASIC3 in the Cortex
and Hippocampus of Epileptic Rats

ASIC3 was expressed in neurons, as shown by coexpression with the neuron marker NSE in the cortex (Fig. 4a) and CA1 region (Fig. 4c). Moreover, Fig. 4b shows the coexpression of ASIC3 with the astrocyte marker GFAP in the cortex. Similarly, we found that ASIC3 was colocalized with GAD67 in the rat cortex (Fig.4d), hippocampal CA1 region (Fig. 4e), and CA3 region (Fig. 4f).

Effect of ASIC3 Inhibition on Seizure Severity

To examine the role of ASIC3 in the progression of epilepsy, we acutely inhibited ASIC3 in rats via an intracerebroventricular injection of the ASIC3 inhibitor APETx2. APETx2 is a potent and selective inhibitor of homomeric ASIC3 channels and ASIC3-containing channels and reversibly inhibits the rat ASIC3 peak current with an $IC_{50}$ of 63 nM, without any effect on the ASIC1a, ASIC1b, ASIC2a, and ASIC2a+3 currents. Additionally, APETx2 displays no neurotoxicity in mice, even after intracisternal injection up to 20 μg [30], and APETx2 has previously been administered at concentrations ranging from 0.022 to 22 μM in vivo [31]. We observed that treatment with APETx2 dramatically shortened the latency to seizure (Fig. 5a) ($P<0.05$), and there were no significant differences between the 5 and 10 μM APETx2 treatment groups ($P>0.05$), according to the results of one-way ANOVA analysis followed by Tukey's HSD post hoc multiple comparison test. Furthermore, blockade of ASIC3 with APETx2 increased the incidence of generalized tonic clonic seizure (GTCS) following pilocarpine injection compared to the control group (Fig. 5b) ($P<0.05$), with no significant differences between the 5 and 10 μM group ($P>0.05$) according to Fisher's exact test. In addition, the Racine score for each 10-min interval was recorded; during the first 10 min after injection, all four groups had similar seizure scores, although rats treated with APETx2 developed more severe seizures over time (Fig. 5c) ($P<0.05$), which confirmed that ASIC3 reduced epilepsy severity. For these
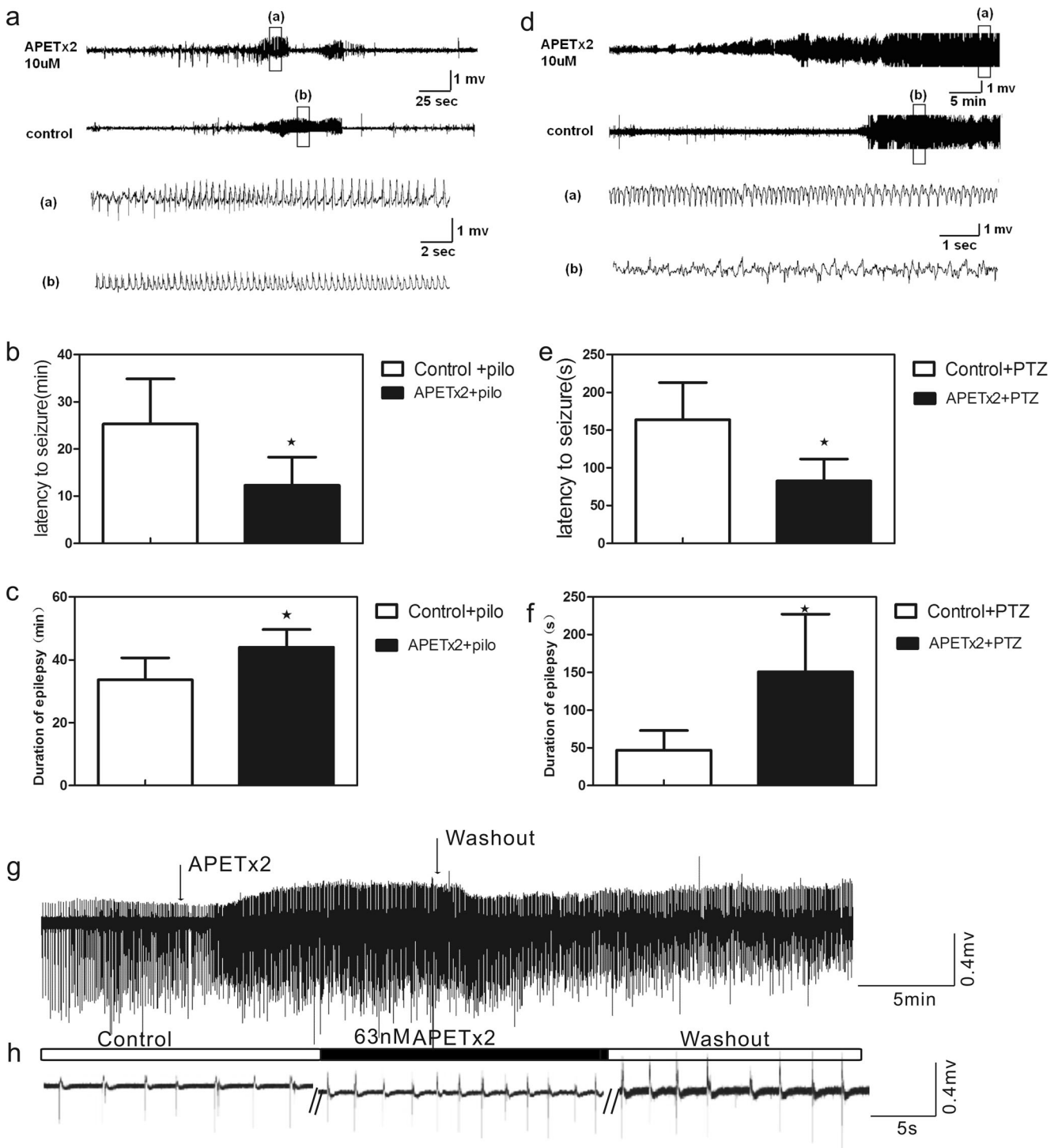
**Fig. 6** Effect of APETx2 on local field potential (LFP). **a**, **d** Typical trace of LFP on rats treated with APETx2. **b**, **e** APETx2 significantly shortened the latency to seizure compared to the controls in a model of pilocarpine-induced (**b**) and PTZ-induced (**e**) seizures ($n=5$, ★$P<0.05$). **c**, **f** The duration of seizure last longer on rats treated with APETx2 in a model of pilocarpine-induced (**b**) and PTZ-induced (**e**) seizures ($n=5$, ★$P<0.05$). **g** APETx2 reversibly increases amplitude and frequency of interictal-like of epileptiform activity in hippocampal slice. The averaged frequency of interictal-like events was elevated from 0.23 to 0.5 Hz, and amplitude was increased from about 0.75 to 1 mV. **h** Expanded view of **g** before (control), during (APETx2), and after (washout) the application of APETx2

comparisons, an ANOVA with repeated measures was used. Moreover, rats injected with APETx2 presented decreased latency to seizure in a model of PTZ (Fig. 5d), further confirming that ASIC3 had anti-epileptic effects. Epilepsy is characterized by synchronized discharges of a population of neurons simultaneously, so we further used an in vivo
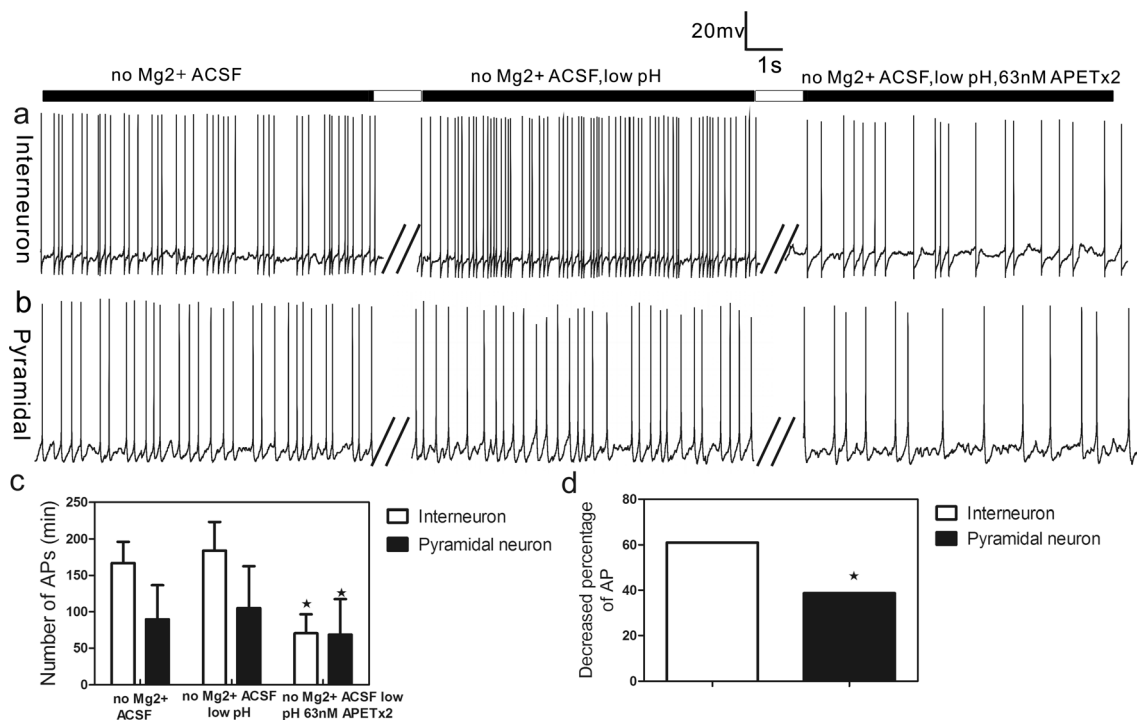
**Fig. 7** Effect of the ASIC3 inhibitor on neuronal excitability. **a**, **b** Typical image of an AP at no Mg$^{2+}$ ACSF, low pH without Mg$^{2+}$ and in perfusion slices treated with 63 nM APETx2 under the same conditions in interneurons and pyramidal neurons. **c** After perfusion, slices treated with APETx2 showed significantly decreased AP firing frequency in interneurons and pyramidal neurons in comparison to the control ($n=5$) (★$P<0.05$). **d** Significantly decreased AP frequencies of interneurons was detected than that of pyramidal neurons ($n=5$) (★$P<0.05$)

multichannel electrophysiological recording to record the effect of APETx2 on LFP. The typical changes of LFP after perfusion with APETx2 are shown in Fig. 6a, d. We observed that treatment with APETx2 dramatically shortened the latency to seizure (Fig. 6b) ($P<0.05$) and prolonged the duration of seizure (Fig. 6c) ($P<0.05$) in a model of pilocarpine-induced seizures. Moreover, we verified the results in PTZ-induced seizures. Rats injected with APETx2 presented decreased latency to seizure in a model of PTZ (Fig. 6e) ($P<0.05$) while prolonged duration of seizure (Fig. 6f) ($P<0.05$) further confirming that ASIC3 had anti-epileptic effects according to the results of independent samples $t$ test. The result of LFP on brain slices supported our idea. APETx2 reversibly increased amplitude and frequency of interictal-like of eplileptiform activity in hippocampal slice (Fig. 6g, h). Our results further demonstrated ASIC3 may have anti-epilepsy function.

### Effect of APETx2 on and Neuronal Excitation, PPR, and mIPSCs

We used the whole cell patch-clamp technique to further characterize the function of ASIC3 in epilepsy. The typical changes in the APs of interneurons and pyramidal neurons after perfusion with APETx2 are shown in Fig. 7a, b. In addition, brain slices perfused with 63 nM APETx2 demonstrated significantly decreased AP frequencies of both interneurons and pyramidal neurons (Fig. 7c) ($P<0.05$), according to the results of

paired samples $t$ tests. Morever, significantly decreased AP frequencies of interneurons was detected than that of pyramidal neurons (Fig. 7d) ($P<0.05$), according to the results of independent samples $t$ test. However, we still do not know the function via presynaptic or postsynaptic. To prove the inhibition, we conducted PPR and mIPSC experiments. We found brain slices perused with 63 nM APETx2 demonstrated no significant difference compared to the control on PPR (Fig. 8a, b) ($P>0.05$) according to the results of paired samples $t$ tests. The results indicated that the inhibition of ASIC3 on epilepsy may via postsynaptic. Figure 8c showed the typical changes of mIPSCs after perfusion with APETx2, APETx2 + bicuculline or bicuculline. After blocking ASIC3 by APETx2, the amplitude of mIPSCs showed significantly decreases compared with the control (Fig. 8d) ($P<0.05$), while the APETx2 group showed no differences with the APETx2 + bicuculline group and the bicuculline group (Fig. 8d) ($P>0.05$). The cumulative fraction of mIPSC amplitude (Fig. 8e) proves the results. Furthermore, the trace of frequencies is the same (Fig. 8f, g). For these comparisons, one-way ANOVA followed by Turkey's HSD post hoc multiple comparison tests.

## Discussion

The data presented here are the first to confirm that ASIC3 is expressed in the temporal cortex and hippocampus of the
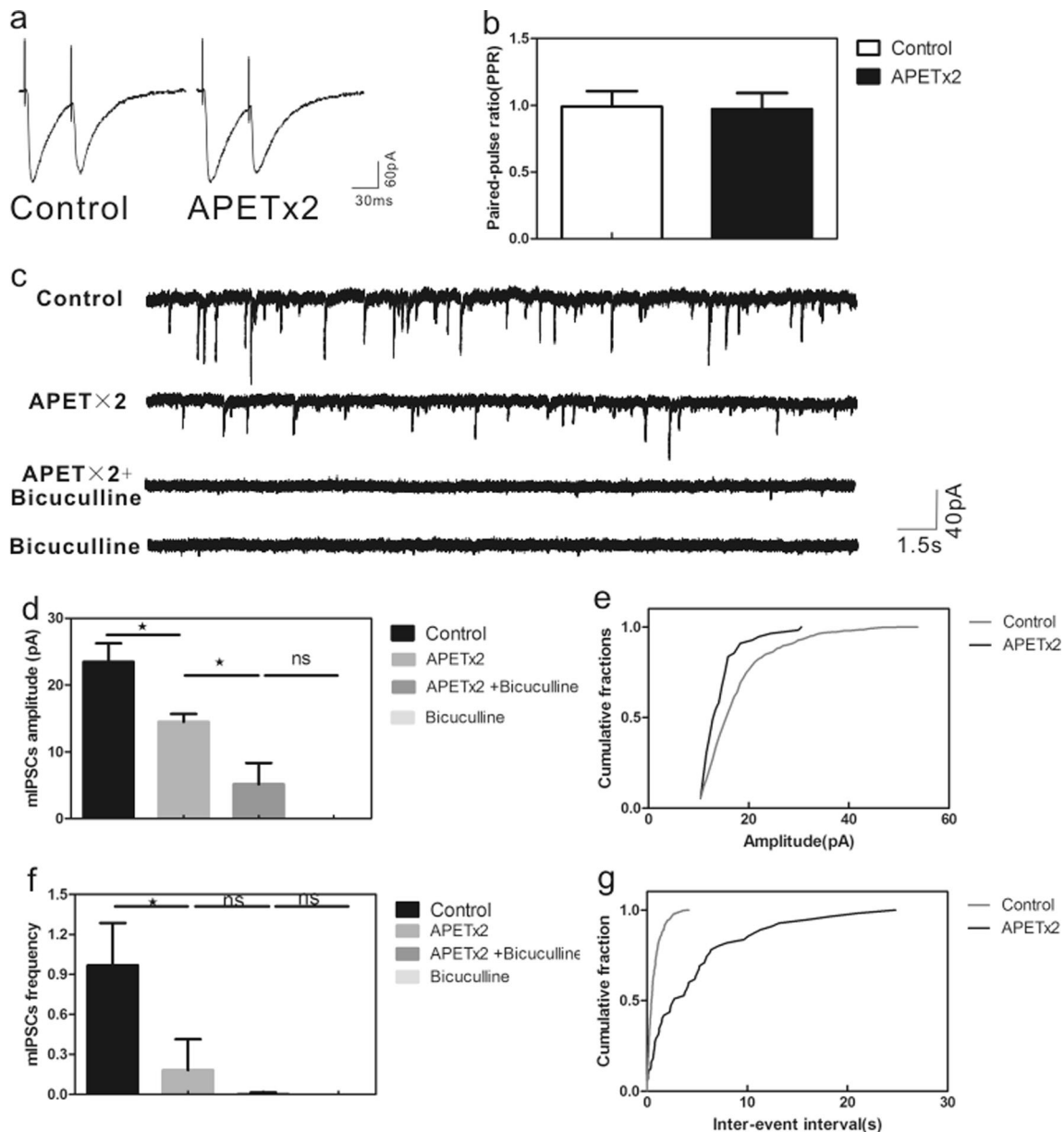
**Fig. 8** Effect of APETx2 on miniature PPR and IPSCs (mIPSCs) in CA1 neurons. **a** Typical image of PPR. **b** PPR showed no significant difference in slices treated with APETx2 in comparison to the control ($n=5$) (★$P>0.05$). **c** Representative traces of mIPSCs in slices in the CA1 region of hippocampal slice. **d** APETx2 significantly decreases the amplitude of mIPSCs in seizure neurons compared with the control ($n=5$, ★$P<0.05$), while showed no differences with the APETx2 + bicuculline group and the bicuculline group ($n=5$, ★$P>0.05$). **e, g** Cumulative fraction of mIPSC amplitude and frequency. **f** APETx2 significantly decreases the frequency of mIPSCs in seizure neurons compared with the control ($n=5$, ★$P<0.05$), while showed no differences with the APETx2 + bicuculline group and the bicuculline group ($n=5$, ★$P>0.05$)

human brain. In particular, ASIC3 protein was detected in the cell membrane and cytoplasm of neurons both in the cortex and hippocampus, as well as the CA3, CA2, and CA1 regions of the rat brain. Additionally, ASIC3 was also expressed in astrocytes, which is accordance with a recent study reporting that ASIC3 is expressed in both cultured astrocytes and in vivo brain tissues [32]. However, we detected ASIC3 expression in the soma of astrocytes but not the dendrites. Accumulating evidence suggests cell-type-specific expression

of acid-sensing ion channels in hippocampal interneurons [33]. Indeed, we found that ASIC3 was colocalized with the GABAergic interneuron marker GAD67 [34] in both the temporal cortex and hippocampus; however, there was no 100 % colocalization between ASIC3 and GABAergic interneurons, which implies that ASIC3 is also expressed in excitatory cells. ASIC3 protein presented an elevated expression pattern in the temporal cortex of TLE patients, and decreased ASIC3 mRNA levels were detected in TLE patients compared

to controls, which was similar to a previous result found in the rat brain showing that ASIC1a and ASIC2b mRNA levels were decreased in different hippocampal areas during pilocarpine-induced SE [35]. The lithium-pilocarpine rat model has also shown similar patterns of epilepsy and molecular–neuropathological alterations as compared to human TLE [36], and the elevated level of ASIC3 expression in the epileptic cortices and hippocampus after pilocarpine-induced seizures provides additional data to support the notion that ASIC3 is involved in epilepsy.

However, the role of ASIC3 in epilepsy remains unknown. We treated rats with the ASIC3 inhibitor APETx2 to evaluate its function in the progression of epilepsy. PTZ kindling is the most widely accepted animal model for studying the effects of novel anti-epileptic molecules [28]. Therefore, we treated rats with APETx2 prior to PTZ kindling and found that blockade of ASIC3 shortened the latency to seizure and increased the incidence of induced GTCS in rats, which indicated that inhibition of ASIC3 increased the severity of epileptic seizures. Moreover, we obtained identical results in a model of pilocarpine-induced seizures, as rats treated with APETx2 developed more severe seizures over time. These results are also similar to findings on the role of ASIC1a, as disruption of the ASIC1a gene or pharmacological inhibition of ASIC1a was shown to increase seizure severity, whereas overexpression of ASIC1a has the opposite effect [37].

The brain pH reduces from 7.35 to 6.8 in epileptic conditions through lactic acid production, $CO_2$ accumulation, and other mechanisms [38, 39]. Study indicated acidosis has effect in seizure inhibition both in patients with epilepsy and brain slices [40, 41]. However, the method which acidosis inhibits seizures is still unknown. The ability of extracellular acidosis to activate the ASICs suggests that these proteins might also mediate the effects of pH on seizures. Our results indicate that ASIC3 may play a role in inhibiting epilepsy, although its underlying mechanism remains unknown. Many studies have shown that GABAergic inhibitory interneurons in the hippocampus have larger ASIC currents than glutamatergic excitatory pyramidal neurons [42, 43, 37]. In our study, we found that blocking ASIC3 significantly decreased the frequency of APs in inhibitory neurons and pyramidal neurons. This result indicates that APETx2 inhibits the excitability of inhibitory neurons and pyramidal neurons during epileptic states. Loss of interneuron or decrease excitability of inhibitory neurons triggers epilepsy, while excitability of inhibitory pyramidal neurons prevents epilepsy [44, 45]. Our results further demonstrated that interneurons had significantly decreased AP frequencies than pyramidal neurons, and inhibition of ASIC3 increased the severity of epileptic seizures. The results presented here reveal that ASIC3 may inhibit epileptic seizures by triggering inhibitory interneuron activity, which is similar to the findings of a recent report showing that ASIC1a null mice could not stimulate AP firing in inhibitory neurons and

therefore failed to demonstrate inhibited seizure activity [37]. Changes of the PPR, coefficient of variance, and mIPSC frequency would be consistent with a presynaptic site of action [46]. We found that APETx2 did not significantly alter the PPR, and APETx2 significantly reduced the amplitudes and frequencies of mIPSCs while showed no differences with the APETx2 + bicuculline group and the bicuculline group. Taken together, our data suggest that ASIC3 modulates GABAergic neurons primarily via postsynaptic mechanisms in interneurons [47]

The current study had certain limitations. Due to ethical requirements, we could not obtain normal brain tissue, so the selected relatively normal brain tissue served as the control. Moreover, as there was no selective agonist for ASIC3, we could not directly observe its function in epilepsy. However, the findings described here proposed a new, anti-epileptic function for ASIC3 and that agent that potentiate ASIC3 activity might reduce seizure severity or duration and possibly prevent epilepsy.

## References

1. Vezzani A, French J, Bartfai T, Baram TZ (2011) The role of inflammation in epilepsy. Nat Rev Neurol 7(1):31–40
2. French JA (2007) Refractory epilepsy: clinical overview. Epilepsia 48(Suppl 1):3–7
3. Perucca E, French J, Bialer M (2007) Development of new antiepileptic drugs: challenges, incentives, and recent advances. Lancet Neurol 6(9):793–804
4. Sharma A, Mathur VP (2011) Refractory epilepsy and the ketogenic diet: pathophysiological aspects and possible implications in dental practice. J Indian Soc Pedod Prev Dent 29(3):188–192
5. Pitkanen A, Lukasiuk K (2011) Mechanisms of epileptogenesis and potential treatment targets. Lancet Neurol 10(2):173–186
6. Schmidt D, Loscher W (2005) Drug resistance in epilepsy: putative neurobiologic and clinical mechanisms. Epilepsia 46(6):858–877
7. Waldmann R, Lazdunski M (1998) H(+)-gated cation channels: neuronal acid sensors in the NaC/DEG family of ion channels. Curr Opin Neurobiol 8(3):418–424
8. Chen CC, England S, Akopian AN, Wood JN (1998) A sensory neuron-specific, proton-gated ion channel. Proc Natl Acad Sci U S A 95(17):10240–10245
9. Price MP, Snyder PM, Welsh MJ (1996) Cloning and expression of a novel human brain Na+ channel. J Biol Chem 271(14):7879–7882
10. Lingueglia E, de Weille JR, Bassilana F, Heurteaux C, Sakai H, Waldmann R, Lazdunski M (1997) A modulatory subunit of acid sensing ion channels in brain and dorsal root ganglion cells. J Biol Chem 272(47):29778–29783

11. Waldmann R, Bassilana F, de Weille J, Champigny G, Heurteaux C, Lazdunski M (1997) Molecular cloning of a non-inactivating proton-gated Na+ channel specific for sensory neurons. J Biol Chem 272(34):20975–20978

12. de Weille JR, Bassilana F, Lazdunski M, Waldmann R (1998) Identification, functional expression and chromosomal localisation of a sustained human proton-gated cation channel. FEBS Lett 433(3):257–260

13. Grunder S, Geissler HS, Bassler EL, Ruppersberg JP (2000) A new member of acid-sensing ion channels from pituitary gland. Neuroreport 11(8):1607–1611

14. Waldmann R, Champigny G, Bassilana F, Heurteaux C, Lazdunski M (1997) A proton-gated cation channel involved in acid-sensing. Nature 386(6621):173–177

15. Alvarez de la Rosa D, Canessa CM, Fyfe GK, Zhang P (2000) Structure and regulation of amiloride-sensitive sodium channels. Annu Rev Physiol 62:573–594

16. Sutherland SP, Benson CJ, Adelman JP, McCleskey EW (2001) Acid-sensing ion channel 3 matches the acid-gated current in cardiac ischemia-sensing neurons. Proc Natl Acad Sci U S A 98(2):711–716

17. Yagi J, Wenk HN, Naves LA, McCleskey EW (2006) Sustained currents through ASIC3 ion channels at the modest pH changes that occur during myocardial ischemia. Circ Res 99(5):501–509

18. Immke DC, McCleskey EW (2003) Protons open acid-sensing ion channels by catalyzing relief of Ca2+ blockade. Neuron 37(1):75–84

19. Chen CC, Zimmer A, Sun WH, Hall J, Brownstein MJ (2002) A role for ASIC3 in the modulation of high-intensity pain stimuli. Proc Natl Acad Sci U S A 99(13):8992–8997

20. Hildebrand MS, de Silva MG, Klockars T, Rose E, Price M, Smith RJ, McGuirt WT, Christopoulos H, Petit C, Dahl HH (2004) Characterisation of DRASIC in the mouse inner ear. Hear Res 190(1–2):149–160

21. Connor M, Naves LA, McCleskey EW (2005) Contrasting phenotypes of putative proprioceptive and nociceptive trigeminal neurons innervating jaw muscle in rat. Mol Pain 1:31

22. Meng QY, Wang W, Chen XN, Xu TL, Zhou JN (2009) Distribution of acid-sensing ion channel 3 in the rat hypothalamus. Neuroscience 159(3):1126–1134

23. Zhang M, Gong N, Lu YG, Jia NL, Xu TL, Chen L (2008) Functional characterization of acid-sensing ion channels in cultured neurons of rat inferior colliculus. Neuroscience 154(2):461–472

24. Kwan P, Arzimanoglou A, Berg AT, Brodie MJ, Allen Hauser W, Mathern G, Moshe SL, Perucca E, Wiebe S, French J (2010) Definition of drug resistant epilepsy: consensus proposal by the ad hoc Task Force of the ILAE Commission on Therapeutic Strategies. Epilepsia 51(6):1069–1077

25. Racine RJ (1972) Modification of seizure activity by electrical stimulation. II. Motor seizure. Electroencephalogr Clin Neurophysiol 32(3):281–294

26. Schmittgen TD, Livak KJ (2008) Analyzing real-time PCR data by the comparative CT method. Nat Protoc 3(6):1101–1108

27. Raol YH, Brooks-Kayal AR (2012) Experimental models of seizures and epilepsies. Prog Mol Biol Transl Sci 105:57–82

28. Dhir A (2012) Pentylenetetrazol (PTZ) kindling model of epilepsy. Curr Protoc Neurosci Chapter 9: Unit9 37.

29. Jimenez-Mateos EM, Engel T, Merino-Serrais P, McKiernan RC, Tanaka K, Mouri G, Sano T, O'Tuathaigh C, Waddington JL, Prenter S, Delanty N, Farrell MA, O'Brien DF, Conroy RM, Stallings RL, DeFelipe J, Henshall DC (2012) Silencing microRNA-134 produces neuroprotective and prolonged seizure-suppressive effects. Nat Med 18(7):1087–1094

30. Diochot S, Baron A, Rash LD, Deval E, Escoubas P, Scarzello S, Salinas M, Lazdunski M (2004) A new sea anemone peptide, APETx2, inhibits ASIC3, a major acid-sensitive channel in sensory neurons. EMBO J 23(7):1516–1525

31. Karczewski J, Spencer RH, Garsky VM, Liang A, Leitl MD, Cato MJ, Cook SP, Kane S, Urban MO (2010) Reversal of acid-induced and inflammatory pain by the selective ASIC3 inhibitor, APETx2. Br J Pharmacol 161(4):950–960

32. Huang C, Hu ZL, Wu WN, Yu DF, Xiong QJ, Song JR, Shu Q, Fu H, Wang F, Chen JG (2010) Existence and distinction of acid-evoked currents in rat astrocytes. Glia 58(12):1415–1424

33. Weng JY, Lin YC, Lien CC (2010) Cell type-specific expression of acid-sensing ion channels in hippocampal interneurons. J Neurosci 30(19):6548–6558

34. Freichel C, Potschka H, Ebert U, Brandt C, Loscher W (2006) Acute changes in the neuronal expression of GABA and glutamate decarboxylase isoforms in the rat piriform cortex following status epilepticus. Neuroscience 141(4):2177–2194

35. Biagini G, Babinski K, Avoli M, Marcinkiewicz M, Seguela P (2001) Regional and subunit-specific downregulation of acid-sensing ion channels in the pilocarpine model of epilepsy. Neurobiol Dis 8(1):45–58

36. Majores M, Schoch S, Lie A, Becker AJ (2007) Molecular neuropathology of temporal lobe epilepsy: complementary approaches in animal models and human disease tissue. Epilepsia 48(Suppl 2):4–12

37. Ziemann AE, Schnizler MK, Albert GW, Severson MA, Howard MA 3rd, Welsh MJ, Wemmie JA (2008) Seizure termination by acidosis depends on ASIC1a. Nat Neurosci 11(7):816–822

38. Somjen GG (1984) Acidification of interstitial fluid in hippocampal formation caused by seizures and by spreading depression. Brain Res 311(1):186–188

39. Wang RI, Sonnenschein RR (1955) PH of cerebral cortex during induced convulsions. J Neurophysiol 18(2):130–137

40. Woodbury DM, Rollins LT, Henrie JR, Jones JC, Sato T (1956) Effects of carbon dioxide and oxygen on properties of experimental seizures in mice. Am J Physiol 184(1):202–208

41. Velisek L, Dreier JP, Stanton PK, Heinemann U, Moshe SL (1994) Lowering of extracellular pH suppresses low-Mg (2+)-induces seizures in combined entorhinal cortex-hippocampal slices. Exp Brain Res 101(1):44–52

42. Cho JH, Askwith CC (2008) Presynaptic release probability is increased in hippocampal neurons from ASIC1 knockout mice. J Neurophysiol 99(2):426–441

43. Bolshakov KV, Essin KV, Buldakova SL, Dorofeeva NA, Skatchkov SN, Eaton MJ, Tikhonov DB, Magazanik LG (2002) Characterization of acid-sensitive ion channels in freshly isolated rat brain neurons. Neuroscience 110(4):723–730

44. Toth K, Eross L, Vajda J, Halasz P, Freund TF, Magloczky Z (2010) Loss and reorganization of calretinin-containing interneurons in the epileptic human hippocampus. Brain 133(9):2763–2777

45. Bouilleret V, Loup F, Kiener T, Marescaux C, Fritschy JM (2000) Early loss of interneurons and delayed subunit-specific changes in GABA (A)-receptor expression in a mouse model of mesial temporal lobe epilepsy. Hippocampus 10(3):305–324

46. Zucker RS, Regehr WG (2002) Short-term synaptic plasticity. Annu Rev Physiol 64:355–405

47. Govindaiah G, Wang Y, Cox CL (2010) Substance P selectively modulates GABA (A) receptor-mediated synaptic transmission in striatal cholinergic interneurons. Neuropharmacology 58(2):413–422